THREE-DIMENSIONAL MODELING OF THE HYDROACOUSTIC TO SEISMIC T-PHASE TRANSITION

Catherine D. de Groot-Hedlin, John A. Orcutt
Scripps Institution of Oceanography

Sponsored by The Defense Threat Reduction Agency

Contract # DSWA01-98-0004

ABSTRACT

Plans call for five T-phase stations to be installed as part of hydroacoustic segment of the International Monitoring System (IMS), for use in detecting nuclear explosions in the oceans. The ability to detect T-phase signals at the seismic T-phase stations relies on an understanding of the transition from ocean-borne acoustic energy to seismic energy. Observations of the seismic T-phase indicates that the hydroacoustic energy may convert to either compressional or shear body waves, or to highly-attenuative interface waves that can be observed near the ocean/land boundary. Previous 2-D modeling efforts have shown that T-phase amplitudes depend strongly on the velocity structure of the seafloor and land portion of the propagation path, as well as the depth of the source within the water column. However, Snell's law indicates that 3-D effects, i.e. the angle of incidence to the coast, must also be considered in modeling the acoustic-to-seismic transmission. In this paper, we model upslope propagation of acoustic energy at a sloping wedge using a 3-D finite-difference time-stepping (3D-FDTD) method. We synthesize both vertical and horizontal velocity waveforms for sources at varying angles of incidence to the ocean/land boundary. We investigate the dependence of signal characteristics on both seismic velocities and source direction.

Although the 3-D model simulations are both simple and small-scale, the following conclusions may be made based on this work. For high slopes at the ocean/land interface, T-phase amplitudes on land increase with increasing seafloor slope. This contradicts previous results computed using 2D modeling at lower slope values. T-phase amplitudes on land are strongly dependent on seafloor velocity, with lower amplitudes resulting from higher seafloor velocities. T-phase amplitudes on land drop off rapidly with increasing angle of incidence of the acoustic phase to the shoreline, then level off past the critical angle. For reflected waves recorded on hydrophones, the amplitude ratio of the reflected to the direct acoustic arrivals increases with both increasing angle of incidence at the shorelineand with increasing impedance mismatch between ocean and land.

KEY WORDS: hydroacoustic, T-phase, finite difference time domain (FDTD),modeling

OBJECTIVE:

The hydroacoustic component of the International Monitoring System (IMS) is a sparse network that will ultimately consist of six hydroacoustic stations and five T-phase stations located on oceanic islands or on a continental coastline (as in the case of VIB, in Canada). The main objective of this project is to model hydroacoustic to seismic coupling in order to develop improved methods of interpreting recorded data at T-phase stations. In this paper, we model the 3-D transmission of acoustic energy at a sloping wedge.

T-phase stations are significantly less sensitive than hydrophones to ocean-borne acoustic energy. Furthermore, analysis of data recorded at T-phase stations is considerably more complex than for the corresponding data at hydroacoustic stations due to complications introduced by the coupling of acoustic to elastic energy. Two-dimensional numerical modeling results obtained using a parabolic equation modeling method (de Groot-Hedlin and Orcutt, 2000) and a finite difference modeling (Stevens et.al, 2000, 2001) both suggest that, for a source in the sound channel, the slope of the ocean/land interface is not important in determining the amplitude of the T-phase arrival. However, it was shown that the slope angle is significant for either very deep or shallow sources that excite higher order acoustic modes, since the acoustic to seismic conversion point is further from shore at shallow slopes. In this case, shallow slopes yield lower velocity T-phase arrivals. Two dimensional modeling also indicates that the on-shore velocity model has a significant effect on T-phase amplitudes; a low velocity surface layer results in comparatively high T-phase amplitudes (Stevens et.al, 2000). Furthermore, the partitioning between T- to P- and T- to S-wave coupling has been shown to be strongly dependent on the velocity structure along the slope (de Groot-Hedlin and Orcutt, 1999).

Comparing T-phase arrivals at a seismic station on Ascension Island to corresponding arrivals at the offshore MILS hydrophones, Hanson (1998) noted that the transfer function (i.e. the relative amplitudes recorded at the land-based and hydroacoustic stations) was azimuthally dependent. Although there was some evidence that this result might be due to differences in the underwater portion of the slope of Ascension Island, it was noted that these results were inconclusive as there were too many other variables complicating this result. These variables include varying distances between the seismometer and the acoustic to seismic conversion region, as well as differences in modal structure of the incoming acoustic phases. Recordings of T-phases at stations in northern California also indicated that T-phase amplitudes depend on the azimuth of the acoustic arrival (de Groot-Hedlin and Orcutt, 2001). Arrivals from events near Hawaii arrived at nearly direct incidence to coast and were easily detectable at Berkeley stations; arrivals from French nuclear tests at high grazing angles were mainly deflected from the coast and were thus far less detectable on land.

RESEARCH ACCOMPLISHED

3-D Acoustic Modeling

In this paper, we examine the effects of off-axis scattering to quantify 3-D transmission effects. We use the 3-D finite difference time domain (FDTD) modeling method using a grid staggered in both time and space domains. This method was first developed by Yee (1966) to solve problems in electromagnetism, and has been widely adapted for use in modeling both acoustic and elastic transmission. One difficulty with this method is that it is memory intensive – about 10 grid points per wavelength are required at the highest frequencies in order to maintain adequate numerical accuracy. Another difficulty is that a method of terminating the computation at the grid boundaries is required to eliminate false reflections from the edges of the computational domain. These problems are related in that, without an adequate absorbing boundary condition (ABC), the grid size must be increased to attenuate the false reflections and separate their arrival in time.

To eliminate reflections from outgoing waves at the edges of the computational domain, and thereby model an unbounded region, we introduce a boundary region in which fields are attenuated. We use the perfectly matched layer

(PML) absorbing boundary condition (ABC) introduced by Berenger (1994), which results in absorption over a wide range of angles and frequencies. We modify Berenger's PML ABC by "splitting" the pressure into components p_x, p_y, and p_z, and introducing loss terms in the boundary regions. It can be shown that, for a uniform boundary, the resulting coefficients can be made arbitrarily small (Hastings et.al., 1996). In the simulations that follow, the inhomogeneous medium intersects the edges of the simulation region, however reflections are still negligible.

A schematic diagram of the physical model is shown in figure 1. The entire model consists of 170x175x90 blocks, with each block measuring 25m on a side. The boundary regions each have a thickness of 8 blocks. The water velocity profile used corresponds to the annual average sound speed profile at 53N, 226E (near VIB). An explosive source is located at 400m depth, at the sound channel minimum. Results are shown for 3 slopes: 90°, 45°, and 30°. The slopes are modeled as stair-steps, rather than smooth gradients. However, the roughness scale is about one tenth of a wavelength at the highest frequencies, so scattering effects should be secondary. The sampling rate is every 0.005 seconds, thus we have very high time resolution. In the following computations, we neglect intrinsic attenuation within the main grid in order to simplify the interpretation of the results. The source function is shown in figure 2, and has a 1-7Hz bandwidth.

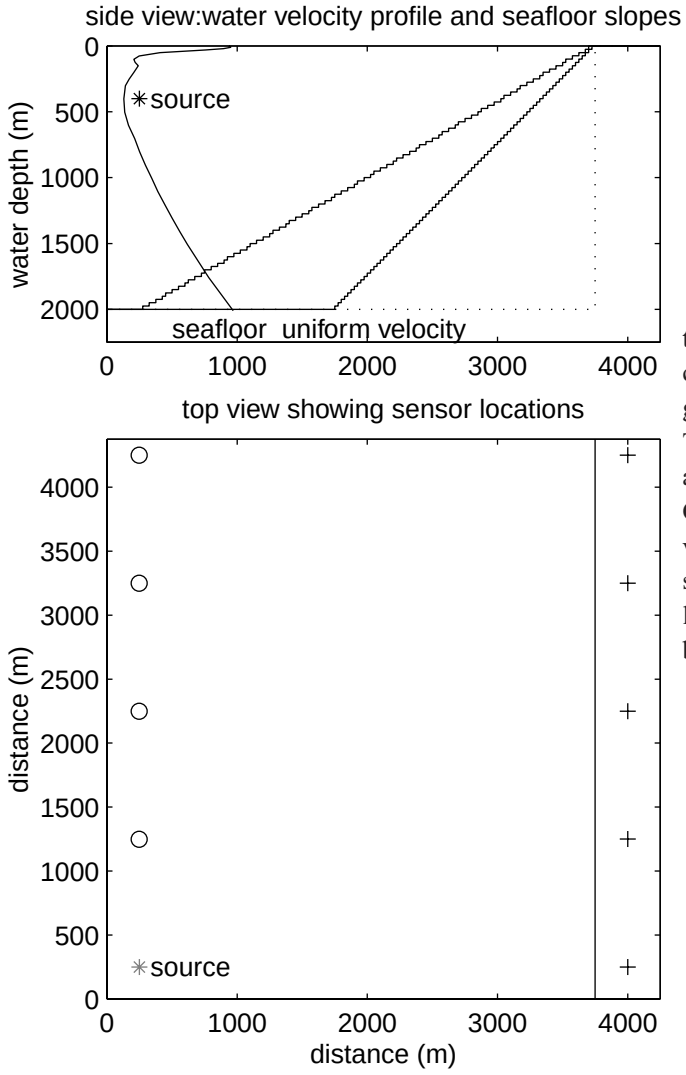

Figure 1. The physical model. a) side view of the model. Velocity and pressure waveforms were computed for 3 slopes: 90°, 45°, and 30°. The gradients are modeled as stair-steps of 25m height. The water velocity profile corresponds to the annual average velocity profile at 53N, 226E, near VIB on Queen Charlotte island. The seafloor is of uniform velocity. b) Top view of the model setup. Pressure sensor locations are indicated by circles; the locations of 3 component seismometers are marked by pluses, and are located 250m inshore.

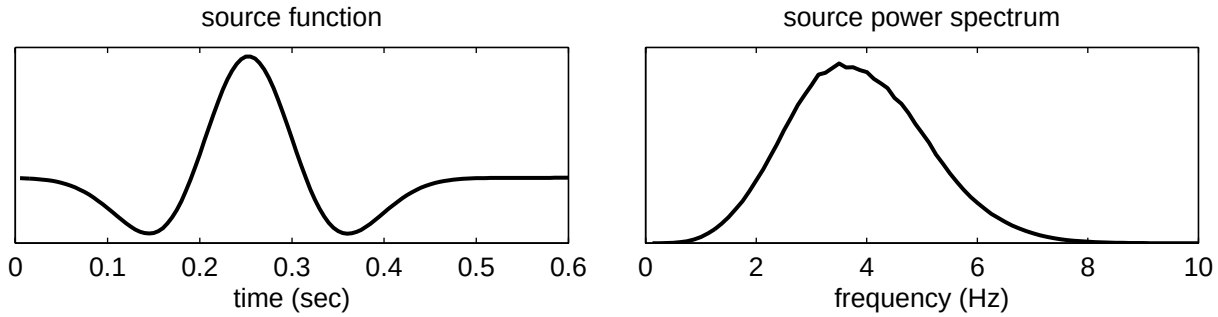

Figure 2. Source function and power spectrum. As shown, the source has a bandwidth from 1-7Hz.

3-D Modeling Results

Top and side views of the pressure field at 1 second, shown in figure 3, indicate how effective the absorbing boundary is. Most absorbing boundaries operate most efficiently at direct incidence, and result in small reflections at other angles. The lack of reflection at the grid boundaries confirms that we can have confidence in the waveform results.

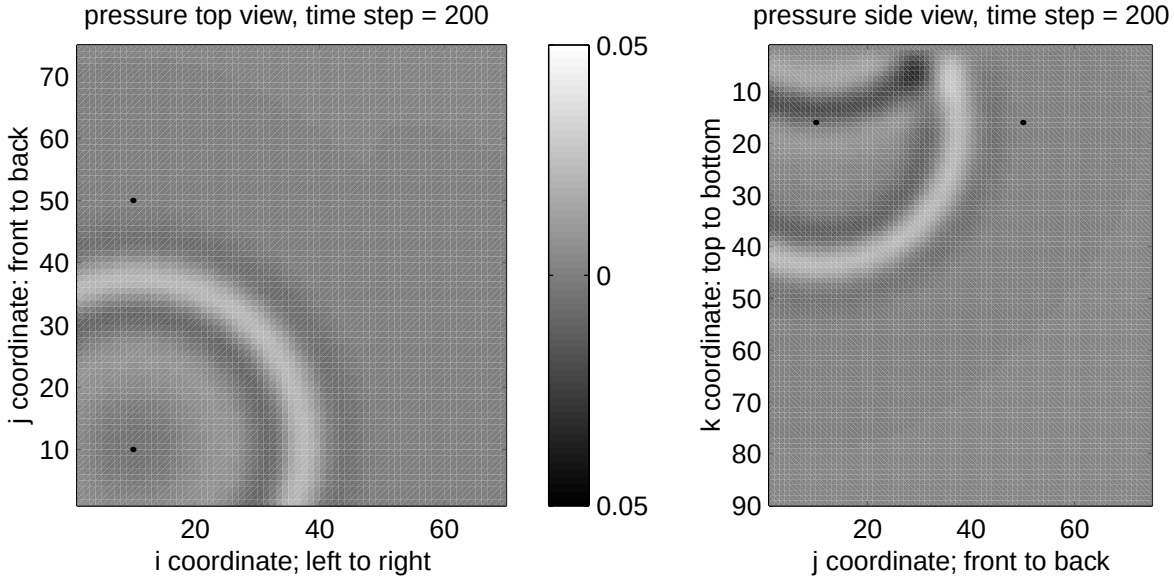

Figure 3. The pressure waveform at t=1 second. No reflections from the grid side boundaries are apparent in the top view (left) or side view cross-section through the receiver location (right). Note that the reflection from the ocean surface, seen in the side view, has the correct (opposite) polarity with respect to the direct arrival. The black dots indicate the location of the source and one of the hydrophones

The velocity waveforms "recorded" at each seismometer location, for each of the three test slopes are shown in Figure 4 slopes for a seafloor velocity of 2500m/sec. The results show that the largest waveforms correspond to the higher slope values. This contradicts previous results which were based on slope values from 2-7^{o} (de Groot-Hedlin and Orcutt, 2000) and 10-30^{o} (Stevens et.al , 2000). Horizontal components of motion have much smaller amplitude for all slope angles, as shown in the results for v_x and v_y. For these models, the variations in amplitude are due to the combined effects of increasing distance and varying angles of incidence at the shoreline. To examine these effects, we plot, in figure 5, the maximum vertical amplitude for each slope values vs. distance from the source. The azi-

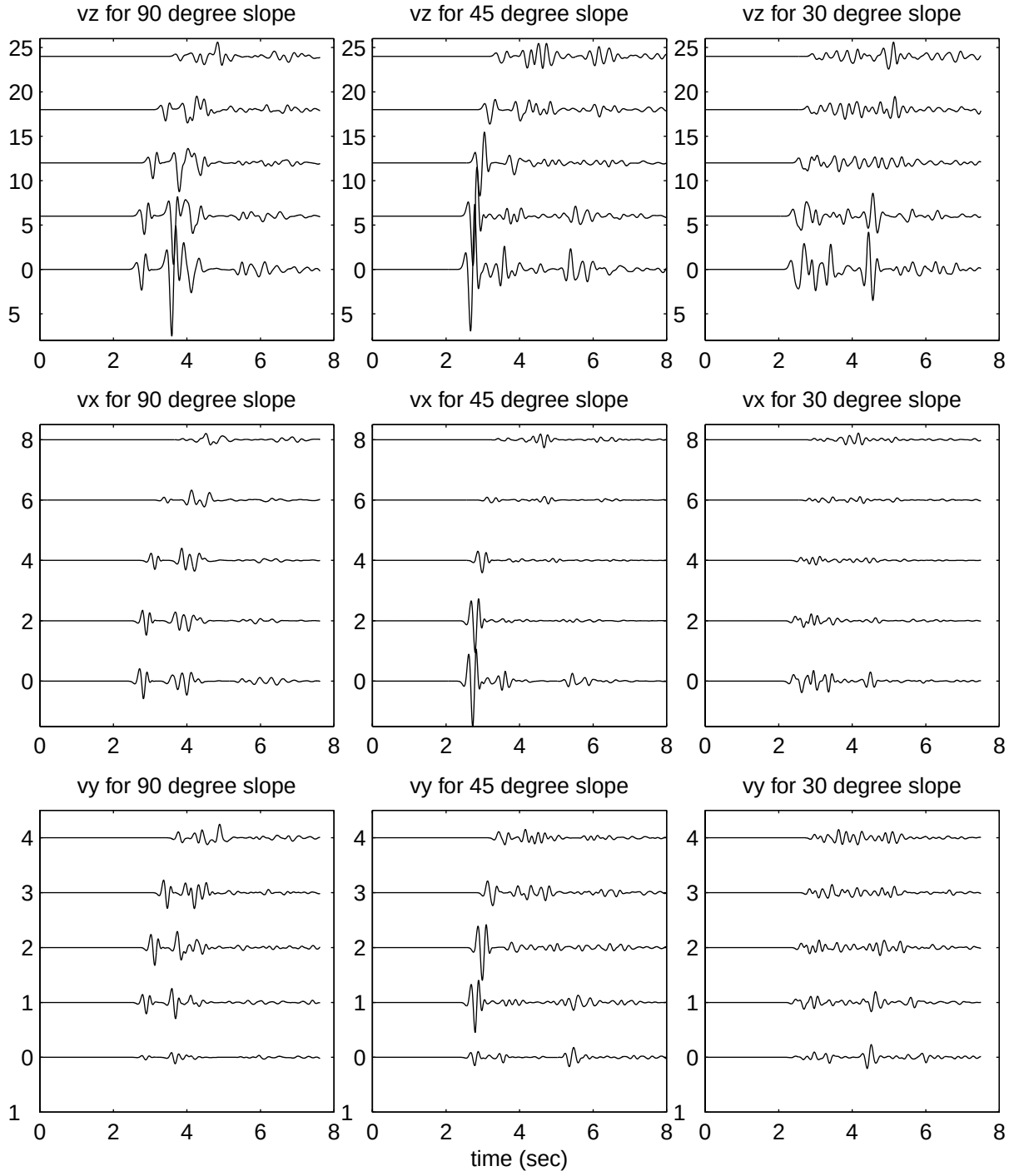

Figure 4. Velocity waveforms for seismometer locations marked by "+" in figure 1. The seafloor velocity in 2500m/sec. Amplitudes are consistent within each direction of motion, ie. amplitudes may be compared between slopes, but note the scale change between components of motion. The distance from the source increases going from bottom to top.

muths from the source to each receiver are also marked. The distance range spans less than a factor of two, yet the amplitudes vary by up to a factor of eight. This suggests that the modeled amplitudes depend more on the azimuth from source to receiver than on the source range. As shown, the amplitude decreases rapidly with increasing azimuth, then levels off at azimuths beyond 39°. The critical angle at this velocity contrast is 31°. For comparison, similar computations were performed for the model with a 45° slope and seafloor velocity of 3500m/sec. Corresponding maximum amplitudes are marked by the triangles in figure 5. Amplitudes are lower at all distance values, and level off at azimuths beyond 28° - the critical angle at this velocity contrast is 23°.

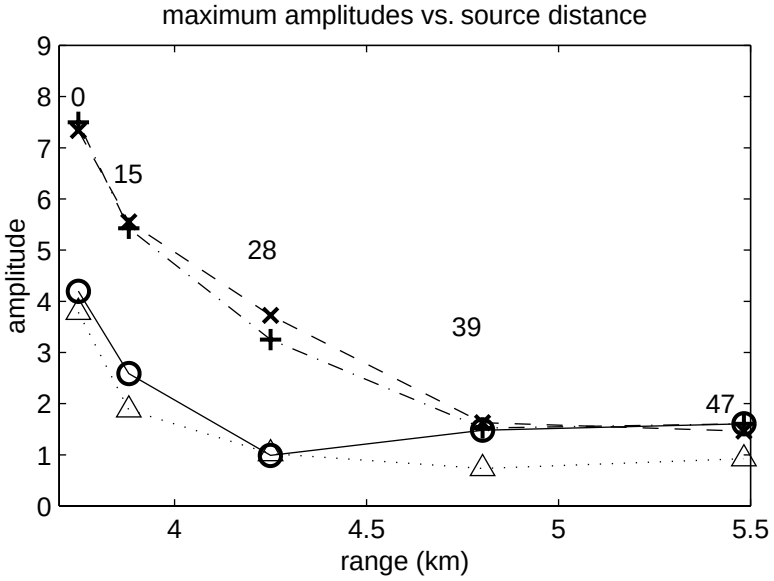

Figure 5. Maximum absolute values of the vertical amplitudes vs. source distance. The back azimuths to the source are also indicated. Results for the 30° slope are indicated by the circles, results for the 45° slope are marked by x'es and the results for the 90° slope are indicated by +'es. For comparison the corresponding results for a model with a 45° slope and a seafloor velocity of 3500m/sec are shown by the gray triangles.

The pressure response at the "hydrophones" at the locations given in figure 1 were derived with no additional computational effort for each model, and are shown in figure 6. The three main wave packets on each waveform correspond to: 1) a combination of the direct and surface reflected arrivals, 2) the reflections from the seafloor at 2.5 to 4 sec, and 3) the reflected arrival from the water/land boundary at 5 to 6 seconds. As expected, the amplitude ratio of the shore-reflected arrival to direct arrival increases with increasing distance from the source (since the reflection coefficient increases with decreasing grazing angle).

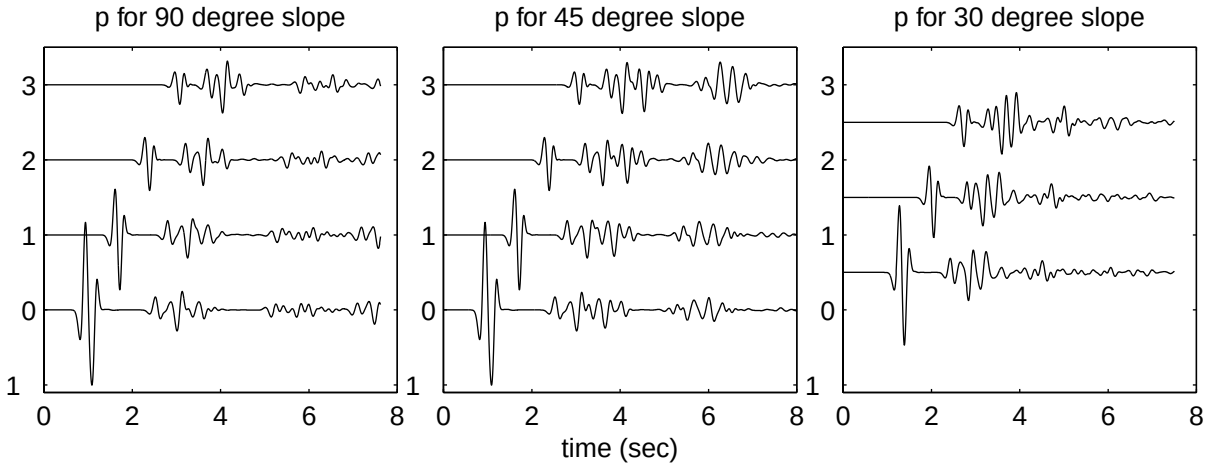

Figure 6. Pressure waveforms for seismometer locations marked by circles in figure 1. For the 30 degree slope, responses were computed at only 3 hydrophones, at locations halfway between those shown in figure 1.

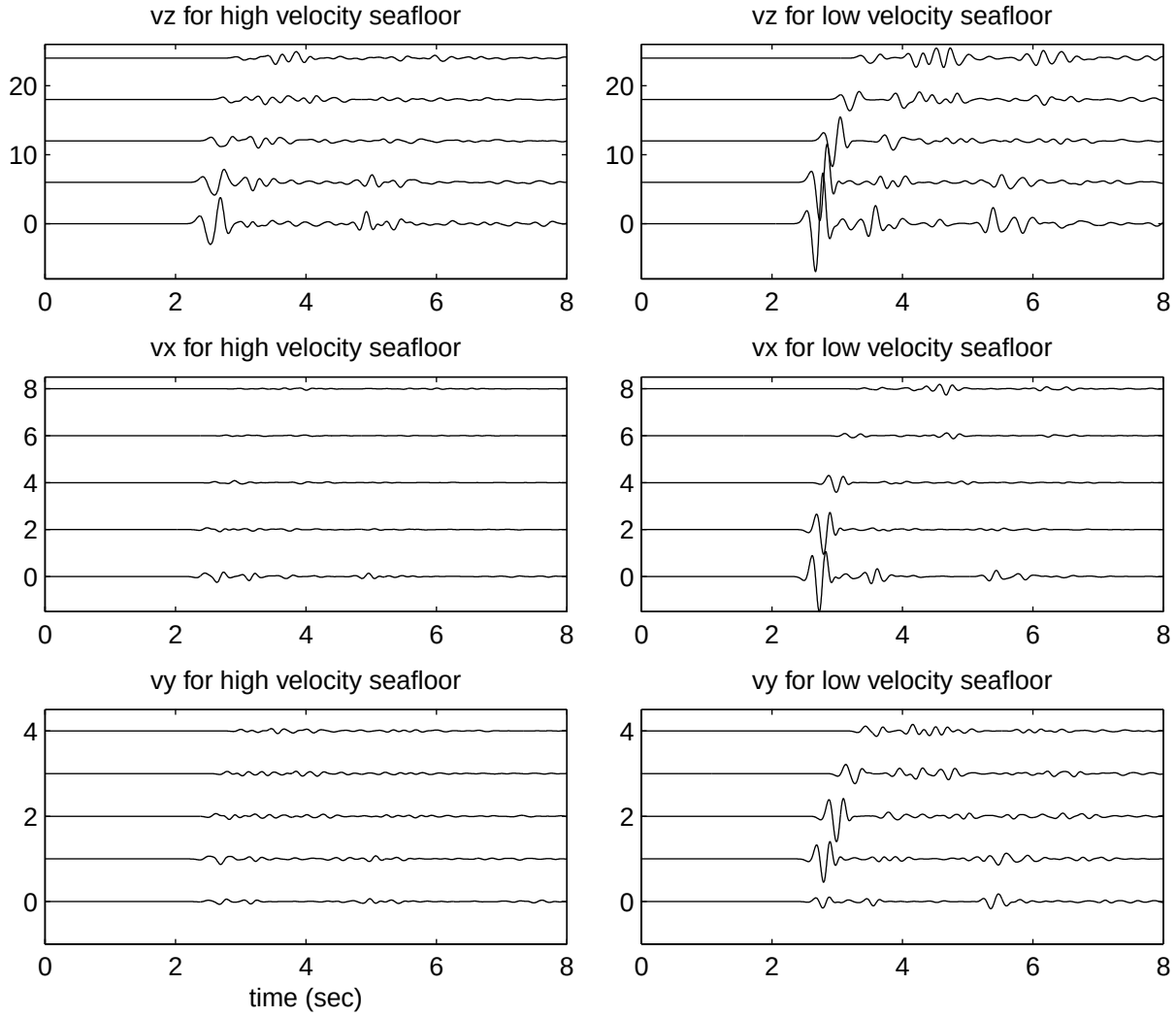

Figure 7. Comparison of velocity waveforms for model with 45° slope and seafloor velocities of 3500m/sec (right) and 2500m/sec (left). T-phase amplitudes are much smaller for the model with the high velocity seafloor.

For comparison, the velocity responses for the model with 45° slope, with a seafloor velocity of 3500m/sec are shown in figure 7. The pressure responses for this model are shown in figure 8. In both figures, these are compared to the previous results for a model with a seafloor velocity of 2500m/sec. Figure 7 shows that the velocities recorded on land are significantly lower for the higher velocity seafloor. As shown in figure 8, the ratio of the reflected arrival to the direct arrival is greater for the larger impedance mismatch.

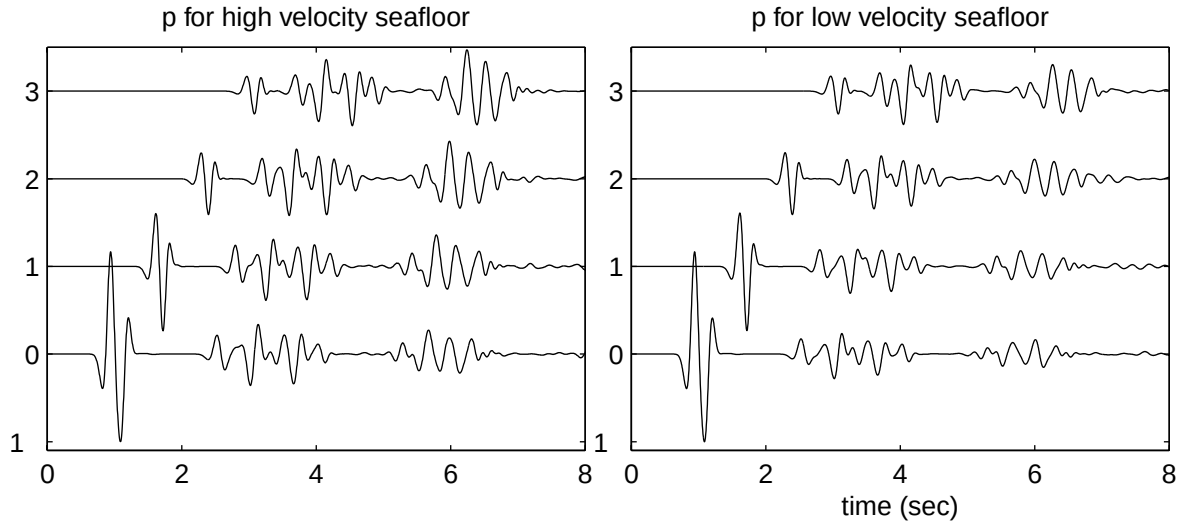

Figure 8. Comparison of pressure waveforms for model with 45° slope and seafloor velocities of 3500m/sec (right) and 2500m/sec (left). Both the seafloor bounce phases (the second arrivals) and the arrivals reflected from the slope (the third arrivals) are larger for the model with the greater velocity contrast.

CONCLUSIONS AND RECOMMENDATIONS

Although the 3-D model simulations are, by necessity, both simple and small-scale, the following conclusions may be made based on this work.

-T-phase amplitudes on land increase with increasing seafloor slopes. This contradicts previous results computed using 2D modeling at lower slope values.
-T-phase amplitudes on land are strongly dependent on seafloor velocity, with lower amplitudes resulting from higher seafloor velocities.
- T-phase amplitudes on land drop off rapidly with increasing angle of incidence of the acoustic phase to the shoreline, then level off past the critical angle.

For reflected waves recorded on hydrophones, the amplitude ratio of the reflected to direct arrivals

-increases with increasing angle of incidence at the shoreline
-increases as impedance mismatch between ocean and land increases

However, this ratio has a complicated dependence on slope at which the acoustic phase is reflected. Reflections have higher amplitude at 45^{o} than at both the 90^{o} and 30^{o} slopes.

These conclusions hold for sources located in the sound channel minimum, and for models with no intrinsic attenuation in the land portion of the travel path. Further work needs to be done using elastic modeling.

References:

Berenger, J.-P., "A perfectly matched layer for the absorption of electromagnetics waves", *J. Comput. Phys*., **114**, 185-200, 1994.

de Groot-Hedlin, C, and J. Orcutt, Comparison of T-phase observations at northern California Seismic Stations and the Pt. Sur hydrophone, 21st annual seismic research symposium, 1999.

de Groot-Hedlin, C, and J. Orcutt, Detection of T-phases at Island seismic stations: dependence on seafloor slope, seismic velocity, and reoughness, 22nd annual seismic research symposium, New Orleans, 2000.

de Groot-Hedlin, C, and J. Orcutt, T-phase observations in northern California; Acoustic to seismic coupling at a weakly elastic boundary, *PAGEOPH*, **158**, 513-530, 2001.

Hastings, F.D., J.B. Schneider, and S.L. Broschat, "Application of the perfectly matched layer (PML) absorbing boundary condition to elastic wav propagation*", J.Acoust.Soc.Am.*, **100**, 3061-3069, 1996.

Hanson, J.A., Seismic and hydroacoustic investigations near Ascension Island, University of Califoria, San Diego, 1998.

Stevens, J.L., G.E. Baker, H. Xu, G. D'Spain, and L.P. Berger, Finite difference modeling of T-phase propagation from ocean to land, 22nd annual seismic research symposium, New Orleans, 2000.

Stevens, J.L., G.E. Baker, R.W. Cook, G.L. D'Spain, L.P. Berger, and S.M. Day, Empirical and numerical modeling of T-phase propagation from ocean to land, *PAGEOPH*, **158**, 531-565, 2001.

Yee, K.S., "Numerical solution of initial boundary value problems involving Maxwell's equation in isotropic media", *IEEE Trans. Antennas Propagat*. **AP-14**, 302-307, 1966.